Dendritic cells from the human female reproductive tract rapidly capture and respond to HIV

M Rodriguez-Garcia[1], Z Shen[1], FD Barr[1], AW Boesch[2], ME Ackerman[2], JC Kappes[3,4], C Ochsenbauer[3] and CR Wira[1]

Dendritic cells (DCs) throughout the female reproductive tract (FRT) were examined for phenotype, HIV capture ability and innate anti-HIV responses. Two main CD11c$^+$ DC subsets were identified: CD11b$^+$ and CD11b^{low} DCs. CD11b$^+$CD14$^+$ DCs were the most abundant throughout the tract. A majority of CD11c$^+$CD14$^+$ cells corresponded to CD1c$^+$ myeloid DCs, whereas the rest lacked CD1c and CD163 expression (macrophage marker) and may represent monocyte-derived cells. In addition, we identified CD103$^+$ DCs, located exclusively in the endometrium, whereas DC-SIGN$^+$ DCs were broadly distributed throughout the FRT. Following exposure to GFP-labeled HIV particles, CD14$^+$ DC-SIGN$^+$ as well as CD14$^+$ DC-SIGN$^-$ cells captured virus, with ~30% of these cells representing CD1c$^+$ myeloid DCs. CD103$^+$ DCs lacked HIV capture ability. Exposure of FRT DCs to HIV induced secretion of CCL2, CCR5 ligands, interleukin (IL)-8, elafin, and secretory leukocyte peptidase inhibitor (SLPI) within 3 h of exposure, whereas classical pro-inflammatory molecules did not change and interferon-α2 and IL-10 were undetectable. Furthermore, elafin and SLPI upregulation, but not CCL5, were suppressed by estradiol pre-treatment. Our results suggest that specific DC subsets in the FRT have the potential for capture and dissemination of HIV, exert antiviral responses and likely contribute to the recruitment of HIV-target cells through the secretion of innate immune molecules.

INTRODUCTION

Sexual transmission of HIV is the main route for HIV acquisition in women worldwide.[1] HIV present in semen overcomes the epithelial barrier[2] to reach immune target cells in the female reproductive tract (FRT). As semen moves from the lower to the upper tract, HIV can interact with immune cells at different anatomical locations in the FRT. Because of their location within or beneath the epithelial lining, dendritic cells (DCs) are one of the first immune cells to encounter virus.[3] DCs have the ability to capture and transport virus to lymph nodes, where HIV trans-infection to T cells and infection dissemination is postulated to occur.[4] Alternatively, complete inactivation of HIV following viral contact with DCs could result in the induction of protective immune responses. Although this model has been proposed *in vitro*, little to nothing is known about resident DCs in the upper and lower FRT, the extent to which different subsets exist, and their roles in HIV acquisition.

Each anatomical region of the FRT displays distinct histological, immunological, and functional characteristics.[5] The lower FRT (ectocervix (ECX) and vagina), lined by stratified squamous epithelial cells, is colonized by commensal microbes and is the site for reception and accumulation of semen. In contrast, the upper FRT (uterine endocervix (CX) and endometrium (EM)) is lined by a single layer of columnar epithelium, has low levels of commensals and has adapted to support implantation and pregnancy.[5] As an example of immune compartmentalization, we recently demonstrated fundamental differences in Th17 CD4$^+$ T-cell distribution and susceptibility to HIV infection in the FRT.[6] Th17 CD4$^+$ T cells, critical components of mucosal surfaces colonized by commensals,[7] were more abundant in CX and ECX compared with the EM of premenopausal women. In addition, we found that CD4$^+$ T cells from ECX were the most susceptible to HIV infection *in vitro,* whereas HIV infection in CD4$^+$ T cells from

[1]Department of Physiology and Neurobiology, Geisel School of Medicine at Dartmouth, Lebanon, New Hampshire, USA. [2]Thayer School of Engineering, Dartmouth College, Hanover, New Hampshire, USA. [3]Department of Medicine and UAB Center for AIDS Research, University of Alabama at Birmingham, Research Service Birmingham, Birmingham, Alabama, USA and [4]Birmingham Veterans Affairs Medical Center, Research Service Birmingham, Birmingham, Alabama, USA. Correspondence: M Rodriguez-Garcia (Marta.Rodriguez.Garcia@dartmouth.edu)

Received 7 January 2016; accepted 7 July 2016; published online 31 August 2016. doi:10.1038/mi.2016.72

the EM was barely detectable.[6] DCs are also particularly abundant at mucosal surfaces in contact with microbes, such as the lung, the gut and the genital tract. However, in the case of the FRT, DCs not only specialize to recognize potential invading pathogens but also to tolerate foreign antigens present in sperm and the developing fetus to allow reproduction.[8] Whether FRT immune compartmentalization extends to differences in DC populations is currently unknown. However, taking into consideration the differences in histology, function, microbiome, and hormonal regulation at different locations in the FRT, we hypothesized that DCs may have different roles and display distinct phenotypes.

Unique to the immune system in the FRT is cyclical hormonal regulation that balances protection against infection and tolerance to allogeneic sperm and fetus.[5] Several studies demonstrate that menstrual status alters susceptibility to HIV and other sexually transmitted diseases[5,9–11] and *in vitro* treatment of immune cells with hormones modulates their immune responses and susceptibility to HIV infection.[12–15] Although MoDC innate immune responses are known to be sensitive to sex hormone regulation,[16,17] potential hormonal effects on mucosal DC innate responses in the FRT are unknown.

Despite the critical role of DCs in sexual transmission of HIV and their potential for induction of protective immune responses, very little is known about DC subsets in the FRT and their responses to HIV infection. Most of our knowledge about mucosal DCs is extrapolated from mouse models or from human intestinal or skin DCs, models that are very different from the human FRT regarding function, commensal colonization and hormonal regulation. A few studies have analyzed DCs in the vagina and ECX[18–20] or in decidual tissue as they contribute to pregnancy,[8] but potential differences between DCs at different FRT sites in non-pregnant women and their roles in antiviral immune protection are unknown.

The goals of this study were first to characterize mucosal dendritic cell subsets relevant for HIV acquisition at different anatomical regions in the FRT, and second to define the extent to which DCs exert early innate antiviral responses after HIV exposure and their potential regulation by sex hormones. Data from this study should provide valuable information about the functional contributions of DCs to sexual HIV acquisition.

RESULTS

Two subsets of DCs ($CD11c^+$) are present in the FRT based on CD11b expression

Mononuclear phagocytes at mucosal surfaces represent a heterogeneous population that includes different types of DCs and macrophages.[21] To characterize tissue-resident DCs in the FRT, as detailed in Methods, mixed cell suspensions from digested EM, CX, and ECX were analyzed by flow cytometry (see gating strategy on **Supplementary Figure 1** online). Phenotypic analysis allowed identification of three distinct populations based on CD11c and CD11b expression (**Figure 1a**): $CD11c^+CD11b^+$ (red), $CD11c^+CD11b^{low}$ (yellow) and $CD11c^{low}CD11b^+$ (blue). Each of these three populations displayed differential expression of CD14 and HLA-DR: $CD11c^+CD11b^+$ cells expressed the highest levels of both CD14 and HLA-DR (**Figure 1b**; red); $CD11c^+CD11b^{low}$ cells (yellow) expressed low levels of CD14 and medium levels of HLA-DR; and $CD11c^{low}CD11b^+$ cells (blue) expressed medium levels of CD14 and low HLA-DR, likely representing mucosal macrophages. For our studies, we focused on mucosal DCs, defined as $CD45^+$, $CD11c^{high,}$ and $HLA\text{-}DR^+$ cells[22] (**Figure 1a**, red and yellow populations). Within $CD11c^+$ cells, $CD11b^+$ DCs were significantly more abundant than $CD11b^{low}$ DCs in CX and ECX (**Figure 1c**; $P = 0.01$ and $P = 0.0002$, respectively). As shown in **Figure 1d**, within each tissue, $CD11b^+$ DCs expressed significantly higher levels of CD14 than $CD11b^{low}$ DCs ($P < 0.0001$, $P < 0.01$, and $P < 0.0001$ for EM, CX, and ECX, respectively). More than 80% of $CD11b^+$ DCs corresponded to $CD14^+$ DCs, whereas for the $CD11b^{low}$ DC subset, $CD14^+$ DCs represented $\sim$ 21%, 38%, and 30% in EM, CX, and ECX, respectively. $CD11b^+$ DCs also expressed higher levels of HLA-DR (**Figure 1e**), although the difference with $CD11b^{low}$ DCs was only significant in the EM ($P < 0.01$). Interestingly, phenotypical differences between tissues were found exclusively for $CD11b^{low}$ DCs, which selectively showed reduced expression of CD14 (**Figure 1d**; $P < 0.05$) and $HLA\text{-}DR^{high}$ (**Figure 1e**; $P < 0.05$) in the EM compared with CX and ECX, respectively. There was a trend for $CD11b^{low}$ DCs to be more abundant in EM than CX and ECX, but this difference was not significant (**Figure 1c**). Overall, these studies demonstrate that the dominant population of DCs within the EM, CX, and ECX are $CD11b^+CD14^+$ DCs.

DC-SIGN and CD103 are differentially expressed on DCs from EM, CX, and ECX

To compare for potential regional differences relevant for HIV acquisition, DC-SIGN and CD103 expression were evaluated on DCs from EM, CX, and ECX. DC-SIGN (CD209), is a mannose receptor that mediates HIV capture and transmission from DCs to $CD4^+$ T cells.[4] As seen in **Figure 2a**, DC-SIGN expression was detected on $CD11b^+$ and $CD11b^{low}$ DCs, with no significant differences between subsets. Interestingly, DC-$SIGN^+$ DCs were more abundant in the CX compared with the EM (**Figure 2a**; $P < 0.05$ for $CD11b^+$ DCs and $P < 0.01$ for $CD11b^{low}$ DCs) and the ECX ($P < 0.05$).

CD103 is an integrin that binds to E-Cadherin on epithelial cells and has been described to be involved in antigen sampling and migration to lymphoid tissue in the mouse and human intestine.[22,23] As shown in **Figure 2b**, CD103 was expressed on $CD14^-$ DCs. $CD103^+$ DCs were found almost exclusively in the EM, where they represented $\sim$ 10% of $CD11c^+$ cells (**Figure 2c**; left graph), compared with 2.5% and 1% of the DCs in CX ($P < 0.05$) and ECX ($P < 0.0009$), respectively. The differential expression of CD103 between anatomical locations was specific for DCs, as CD103 expression on T cells from the same donors was not different among sites (**Figure 2c**; right graph). Importantly, $CD103^+$ DCs did not express DC-SIGN (**Figure 2d**), demonstrating that these are distinct cell subsets.

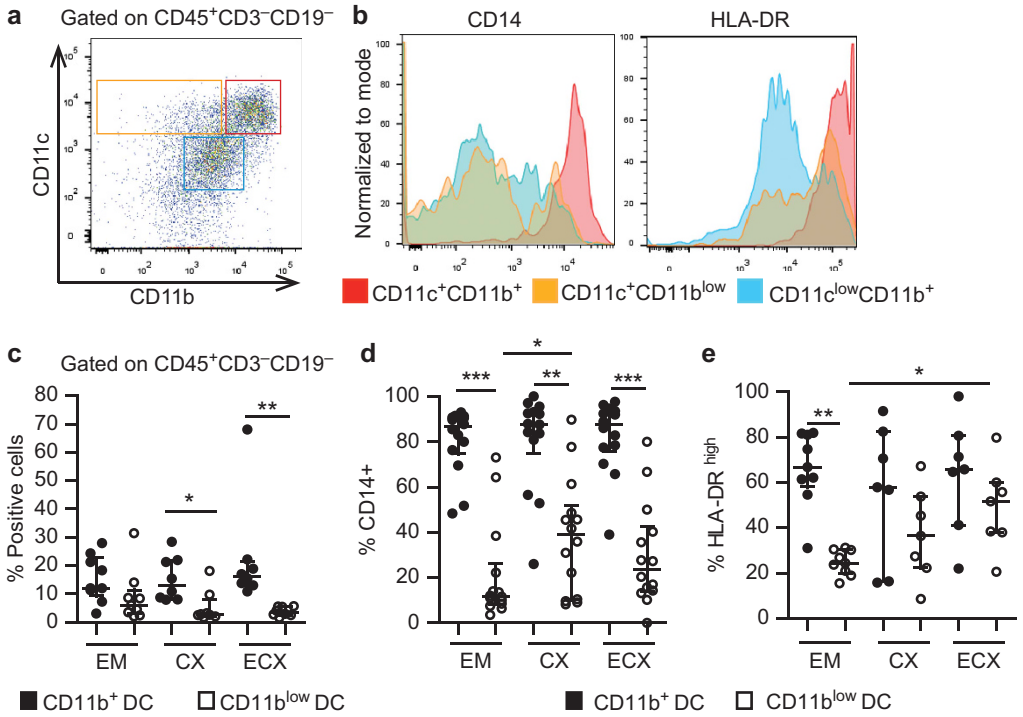

Figure 1 Characterization of CD11c$^+$ DCs in FRT tissues. (**a**) Representative dot plot showing three distinct populations based on CD11c and CD11b expression, after gating on CD45$^+$ immune cells and excluding CD3$^+$ T cells and CD19$^+$ B cells. (**b**) Representative overlay comparing CD14 and HLA-DR expression on the three populations identified in (**a**). (**c**) Percentage of CD11c$^+$CD11b$^+$ DCs (black dots) and CD11c$^+$CD11b^{low} DCs (white dots) in endometrium (EM), endocervix (CX), and ectocervix (ECX) after gating on CD45$^+$CD3$^-$CD19$^-$ cells ($n=9$) (**d**) Expression of CD14 ($n=14$) and (**e**) HLA-DR^{high} ($n=9$) on CD11c$^+$CD11b$^+$ DCs (black dots) and CD11c$^+$CD11b^{low} DCs (white dots) in endometrium (EM), endocervix (CX), and ectocervix (ECX). Each dot represents a single patient; matching EM, CX, and ECX were obtained from each patient. Horizontal lines represent the median ± IQR. Statistical analysis was performed using the non-parametric Kruskal–Wallis test with Dunn's post-test correction for multiple comparisons. *$P<0.05$; **$P<0.01$; ***$P<0.001$.

CD1c is highly expressed on DCs from the FRT

To better characterize FRT DCs and to differentiate between myeloid DCs and Langerhans cells, expression of CD1c and CD207 was determined.

CD1c$^+$ was strongly expressed on DCs from EM, CX, and ECX with >50% of positive cells and no differences between CD11b$^+$ and CD11b^{low} DCs (**Figure 3a**; median of 68% and 57%, respectively). A subset of CD1c$^+$ DCs co-expressed CD14 (**Figure 3b**). As shown in **Figure 3c**, between 20% and 60% of cells co-expressed CD1c and CD14 within the CD11b$^+$ population, whereas co-expression was only 25% or less on CD11b^{low} DCs ($P<0.001$), for which the majority of cells were CD1c$^+$CD14$^-$ ($P<0.0001$).

CD207 (Langerin) was found only on CD1c$^+$ DCs (**Figure 3d**). CD207 expression was low but detectable on both CD11b$^+$ and CD11b^{low} DCs. The highest expression was observed in the EM, with up to 15% of CD207$^+$ cells. However, co-expression of CD1c and CD207 suggests that these cells are of interstitial origin and not Langerhans cells.[24] Neither CD207$^+$ nor CD1c$^+$ DCs co-expressed CD103, suggesting that they represent distinct DC subsets (**Figure 3e**).

Recognizing that tissue macrophages can express CD11c, CD11b, CD14, and HLA-DR, and that ~20–40% of cells within the CD11c$^+$CD11b$^+$ population were CD1c$^-$ (**Figure 3c**), we expanded our phenotypical characterization to include CD163, known to be highly expressed on FRT macrophages.[25] However, CD163 was barely detectable in most of the tissues (**Figure 3f**), suggesting that macrophages were not a major contaminating population.

Overall, these results demonstrate that bona fide CD1c$^+$ myeloid DCs constitute a major population in both CD11b^{low} and CD11b$^+$ cells. However, the presence of CD14$^+$CD1c$^-$ cells that lack macrophage markers (CD163), likely indicate that the CD14$^+$ population represents a mixture of DCs and monocyte-derived cells.

HIV capture is mediated by CD11c$^+$CD14$^+$ cells in EM, CX, and ECX

To evaluate the ability of different DC subsets to capture HIV, mixed cell suspensions were exposed to GFP-labeled HIV-viral-like particles (VLPs) carrying R5Env proteins for 1 h and then analyzed by flow cytometry. R5Env proteins were chosen based on the evidence that mucosal transmission occurs with HIV utilizing CCR5 co-receptor.[26–28] HIV-GFP VLP capture occured throughout the FRT, with no significant differences between anatomical sites (**Figure 4a**). Viral capture was detected exclusively on CD11c$^+$CD14$^+$ cells in EM, CX, and ECX (**Figure 4b**, upper row), but not CD14$^-$ DCs or

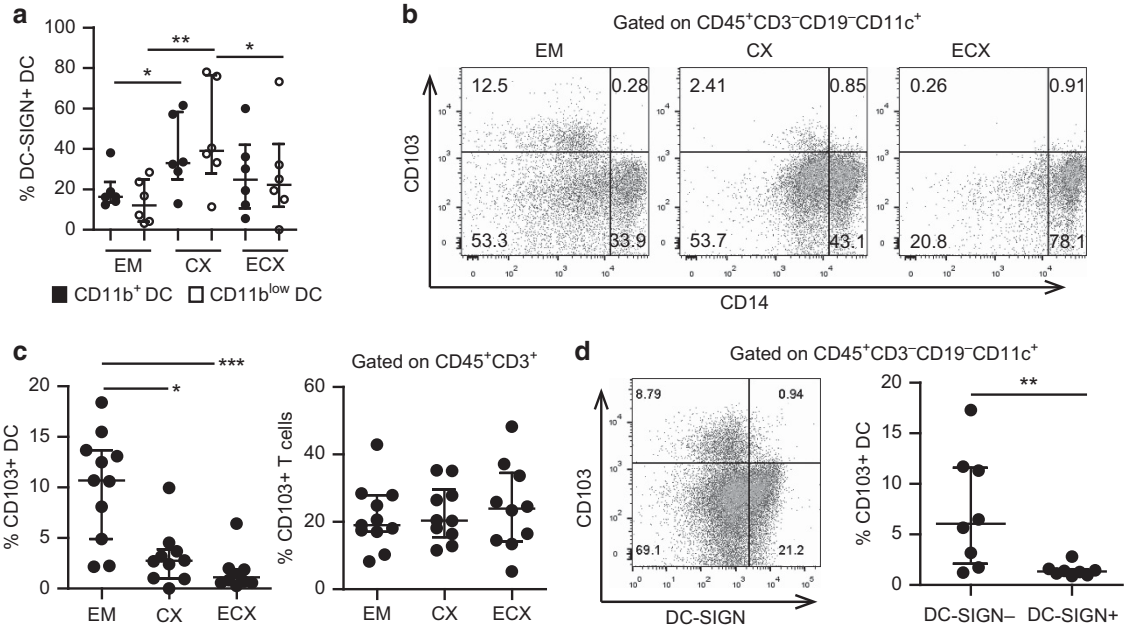

Figure 2 Expression of DC-SIGN and CD103 on DCs from the FRT. (**a**) Percentage of DC-SIGN$^+$ DCs within CD11b$^+$ DCs (black dots) and CD11b^{low} DCs (white dots) in endometrium (EM), endocervix (CX), and ectocervix (ECX). Horizontal lines represent the median ± IQR ($n=6$). (**b**) Representative dot plot of CD103 expression versus CD14 expression on CD11c$^+$ cells from EM, CX, and ECX. (**c**) Percentage of CD103$^+$ DCs in EM, CX, and ECX after gating on CD11c$^+$ cells (left graph) or on CD3$^+$ T cells (right graph). The same patients are shown in both graphs ($n=11$). Each dot represents a single patient; matching EM, CX, and ECX were obtained from each patient. (**d**) Representative dot plot and graph showing the lack of co-expression of DC-SIGN and CD103 on CD11c$^+$ DCs from the EM. Each dot represents a single patient ($n=8$). Horizontal lines represent the median ± IQR. *$P<0.05$; **$P<0.01$; ***$P<0.001$. Statistical analysis was performed using the non-parametric Kruskal–Wallis test with Dunn's post-test correction for multiple comparisons (**a** and **c**) and the non-parametric Mann-Whitney *U*-test (**d**).

CD103$^+$ DCs (**Figure 4b** and **c**). As the majority of HIV-GFP VLPs were captured by CD11c$^+$CD14$^+$ cells, we analyzed CD1c expression to further characterize the nature of the populations with viral capture potential. CD1c was expressed on ~20–30% of HIV-GFP VLP$^+$ cells (**Figure 4d**), indicating that CD1c$^+$ myeloid DCs as well as CD11c$^+$CD14$^+$ monocyte-derived cells have the ability to capture HIV.

Next we explored if HIV capture was mediated by DC-SIGN$^+$ cells. As shown in **Figure 4e**, DC-SIGN$^+$ as well as DC-SIGN$^-$ cells captured HIV-GFP VLPs; however, within HIV-GFP VLP$^+$ cells, the predominant population with capture potential was DC-SIGN$^-$ (**Figure 4f**, white circles). These results suggest that CD103$^+$ DCs and DC-SIGN$^+$ cells are differentially involved in HIV acquisition, and that CD14$^+$CD1c$^+$ DCs with HIV capture potential are present throughout the FRT.

CD1a expression and maturation status of DCs in the FRT

To further characterize DCs in the FRT, we analyzed CD1a expression and maturation status of DCs in the different tissues. As seen in **Figure 5a**, CD11c$^+$ cells could be divided into four subsets according to CD1a and CD14 expression: (i) CD1a$^+$CD14$^-$, (ii) CD1a^{low}CD14^{low}, (iii) CD1a$^-$CD14^{hi}, (iv) CD1a$^-$CD14$^-$. Of these, CD1a^{low}CD14^{low} and CD1a$^-$CD14^{hi} were CD11b$^+$ DCs, CD1a$^+$CD14$^-$ expressed intermediate levels of CD11b and CD1a$^-$CD14$^-$ were CD11b^{low} DCs (**Figure 5b**). The same pattern was observed in EM, CX, and ECX.

Next we assessed maturation status of the different DC subsets and found that HLA-DR and CD86 were expressed on all four subsets (not shown). Using CD83, a well-recognized marker for mature DCs, we found expression on more than 90% of CD1a$^+$CD14$^-$ DCs and ~35% of CD1a^{low}CD14^{low} DCs, with no CD83 detected on CD1a$^-$CD14^{hi} or CD1a$^-$CD14$^-$ DCs (**Figure 5c**; $P<0.0001$).

Upon maturation, DCs are known to upregulate CCR7, which controls the migration of cells to secondary lymphoid organs for antigen presentation.[29] As seen in **Figure 5d**, CCR7 was negative or barely detectable on CD1a$^-$CD14^{hi} and CD1a$^-$CD14$^-$ DCs, in agreement with the absence of CD83 and confirming immature DC state. CCR7 was expressed on CD1a^{low}CD14^{low} and CD1a$^+$CD14$^-$ DCs consistent with increased maturation. However, it is worth noting that CD1a$^+$CD14$^-$ DCs expressed low CCR7 levels relative to their CD83 expression compared to CD1a^{low}CD14^{low} DCs. No significant differences were found for CD83 or CCR7 expression between EM, CX, and ECX for each subset (**Supplementary Figure 2a–b**).

Isolation of DCs from the FRT using CD1a- or CD14-positive magnetic bead selection

We developed a protocol to isolate a purified population of mucosal DCs using positive magnetic bead selection with either

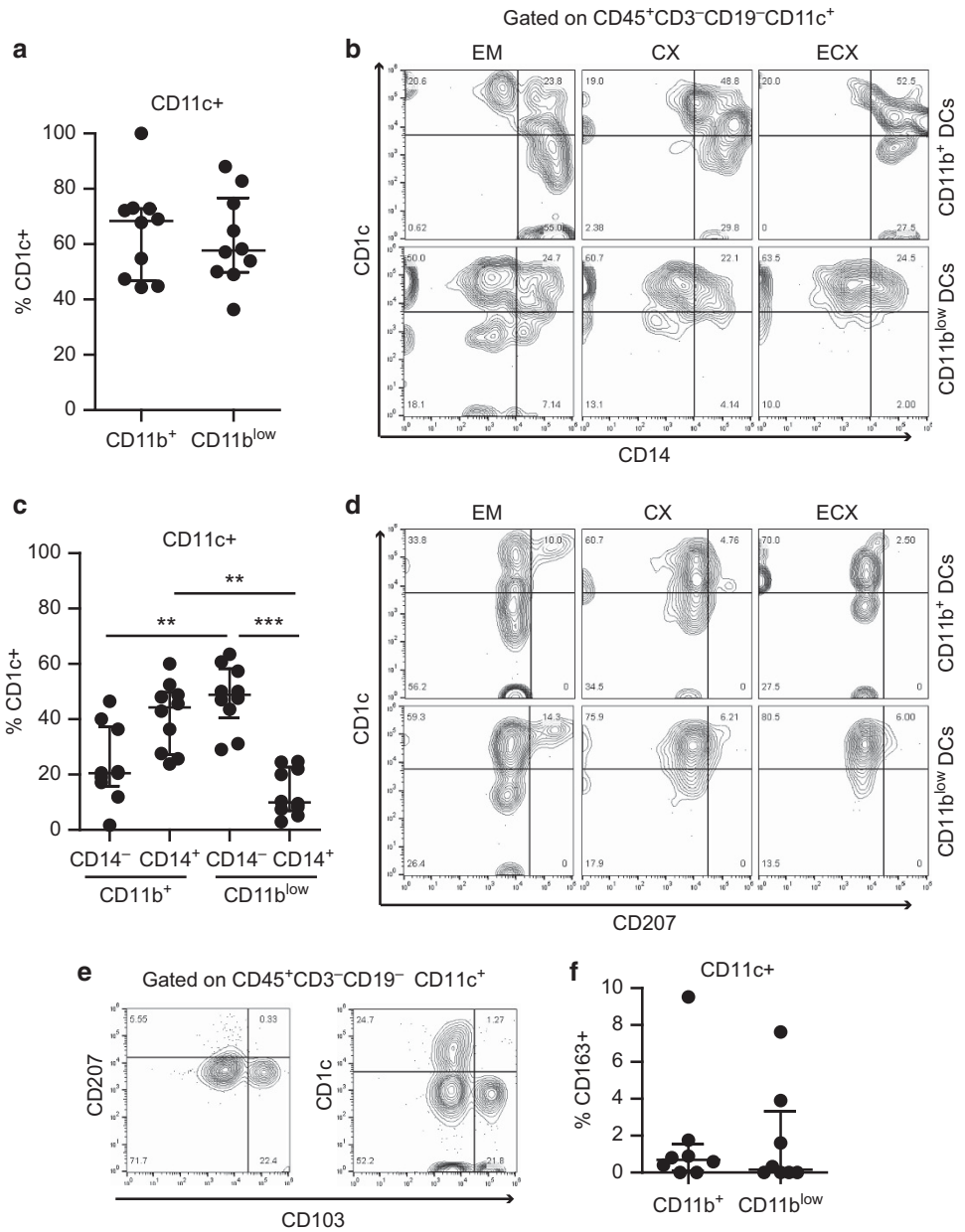

Figure 3 Identification of CD1c$^+$ myeloid DCs in EM, CX, and ECX. (**a**) Percentage of CD1c$^+$ DCs after gating on CD11c$^+$CD11b$^+$ and CD11c$^+$CD11b^{low} cells. (**b**) Representative contour plot of CD14 and CD1c expression on CD11c$^+$ cells from EM, CX, and ECX. Top row shows CD11c$^+$CD11b$^+$ cells and bottom row CD11c$^+$CD11b^{low} cells. (**c**) Percentage of CD1c$^+$ DCs co-expressing or not CD14 after gating on CD11c$^+$CD11b$^+$ and CD11c$^+$CD11b^{low} cells. Statistical analysis was performed using the non-parametric Kruskal–Wallis test with Dunn's post-test correction for multiple comparisons (**d**) Representative contour plot of CD207 and CD1c expression on CD11c$^+$ cells from EM, CX and ECX. Representative of three independent experiments with three different women. (**e**) Representative contour plot of CD103 versus CD207 and CD1c expression on CD11c$^+$ cells from EM, CX, and ECX. Representative of three independent experiments with three different women. (**f**) Percentage of CD163$^+$ DCs after gating on CD11c$^+$CD11b$^+$ and CD11c$^+$CD11b^{low} cells. For a, c and f, dots represent combined results for different tissues from four women (matching EM, CX, and ECX from three women plus one single EM from a different woman). Horizontal lines represent the median ± IQR. $^{**}P<0.01$; $^{***}P<0.001$.

CD1a (**Figure 6a**, top) or CD14 (**Figure 6a**, bottom), to later evaluate anti-HIV responses by DCs from the FRT. As seen in **Figure 6b**, each protocol resulted in a majority of cells that were CD11c$^+$CD11b$^+$. CD1a$^+$ selection provided a homogeneous population with ~90% of selected cells expressing the HIV receptor CD4 and 80% the co-receptor CCR5 (**Figure 6c**, top). CD14$^+$ selected cells were more heterogeneous with ~65% of cells expressing CD4 and 70% CCR5 (**Figure 6c**, bottom). Purity of the population and fluorescence minus one controls are shown in **Supplementary figure 3f, g**.

Selected cells showed dendritic morphology (**Figure 6d**). To further demonstrate that the magnetically selected cells contained a majority of DCs, their ability to stimulate naive T cells was evaluated. After 6 days in co-culture, both mucosal

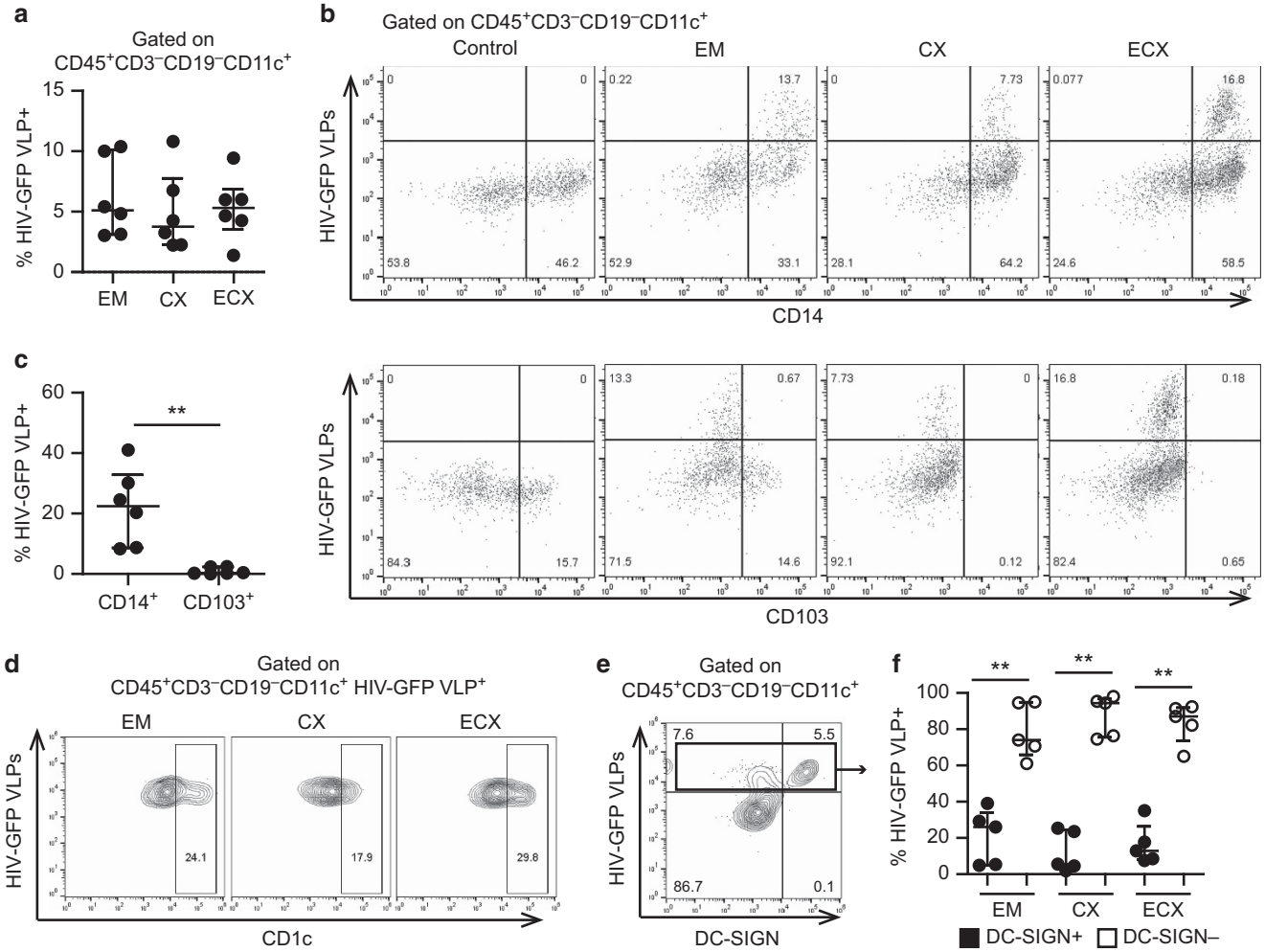

Figure 4 HIV capture by DCs from the FRT. (**a**) Comparison of HIV-GFP VLPs capture by $CD11c^+CD14^+$ cells from the EM, CX, and ECX from six different individuals; matching EM, CX, and ECX were obtained from each patient. (**b**) Mixed cell suspensions from endometrium (EM), endocervix (CX), and ectocervix (ECX) incubated with HIV-GFP VLPs BaL.26 env or media (control) for 1 h. Dot plots show cells gated as $CD45^+$ $CD3^-CD19^-$ $CD11c^+$. Cells that capture the virus appear as GFP^+. Representative result with matched tissues from the same donor. (**c**) Comparison of HIV-GFP VLPs capture by $CD11c^+CD14^+$ cells or $CD103^+$ DCs from the EM ($n=6$). Each dot represents an individual patient. $^{**}P<0.01$. (**d**) Representative contour plot of CD1c expression on HIV-VLP + cells from EM, CX, and ECX. Representative of three independent experiments with three different women. (**e**) Representative contour plot of DC-SIGN and HIV-VLP capture after gating on $CD11c^+$ cells. (**f**) Percentage of DC-SIGN + and DC-SIGN- cells within HIV-GFP VLP^+ cells in EM, CX, and ECX ($n=5$). Matching EM, CX, and ECX were obtained from each patient. Horizontal lines represent the median ± IQR. Statistical analysis was performed using the non-parametric Mann–Whitney *U*-test.

CD1a and CD14 selected cells were able to induce proliferation of allogeneic naive T cells (**Figure 6e**). Proliferation levels were similar to those induced by *in vitro* generated MoDCs used as a control. These results indicate that a significant proportion of selected cells display DC functions.

Secretion of cytokines and chemokines by FRT DCs in response to HIV stimulation

To characterize the early responses to HIV by FRT DCs, $CD14^+$-selected cells from EM, CX, and ECX were stimulated with HIV-BaL for 3 h and secretions analyzed for the presence of a selected panel of cytokines and chemokines by luminex assay. To mimic mucosal transmission[26–28] HIV-BaL was selected as a well-defined CCR5 co-receptor utilizing HIV reference strain, given that low cell availability prevented us from using a panel of bona fide transmitted/founder strains.

As shown in **Figure 7**, CCL2 (MCP-1: twofold increase) and CCR5 ligands (CCL3: twofold increase and CCL4: fourfold increase) were significantly upregulated in response to HIV challenge. There was a modest but significant increase in interleukin (IL)-8 secretion (1.3-fold). In contrast, classical pro-inflammatory cytokines (IL-6, IL-1β, tumor necrosis factor-α) were not modified within 3 h of viral exposure. Importantly, interferon-α2, IL-1α, and IL-10 were undetectable or barely detectable before and after the 3 h challenge. No significant differences were found between tissues, except for a trend toward higher constitutive production of these molecules in ECX relative to that seen in EM and CX.

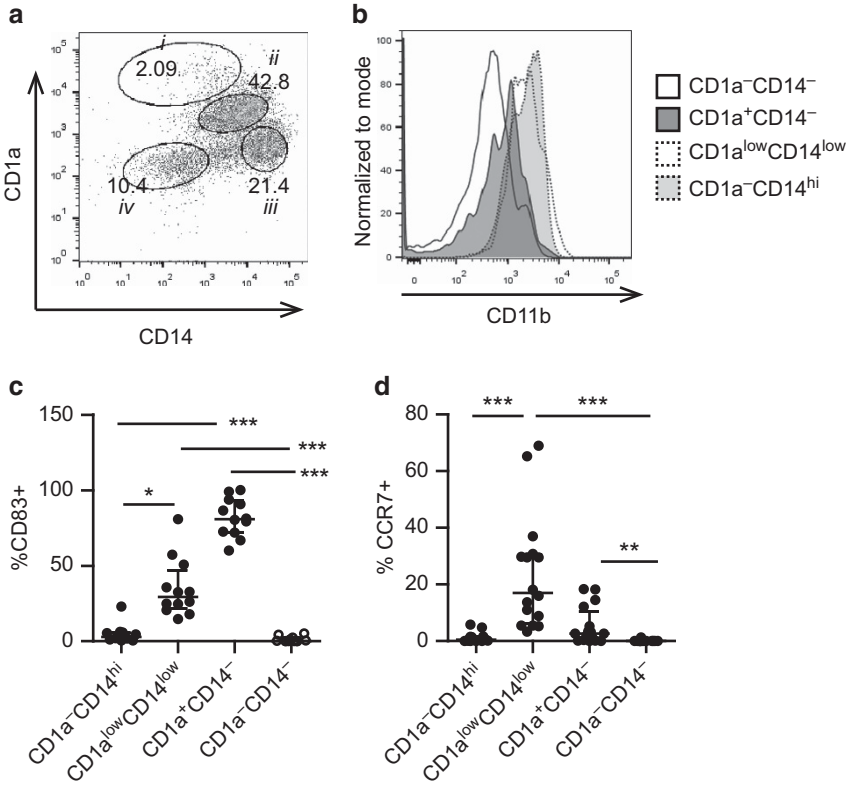

Figure 5 CD1a expression and maturation of DCs in the FRT. (**a**) Representative dot plot showing expression of CD1a and CD14 (gated on $CD45^+$, $CD3^-$ $CD19^-CD11c^+$) and (**b**) overlay of CD11b expression in the different populations. (**c**) Percent of $CD83^+$ and (**d**) $CCR7^+$ DCs on $CD1a^-CD14^{hi}$, $CD1a^{low}CD14^{low}$, $CD1a^+CD14^-$ and $CD1a^-CD14^-$ cells. Dots represent combined results for the different tissues from five women for CD83 (matching EM, CX, and ECX from four women plus one single EM from a different woman) and from eight women for CCR7 (matching EM, CX, and ECX from four women and single EM from four women). Horizontal lines represent the median ± IQR. $^*P<0.05$; $^{**}P<0.01$; $^{***}P<0.001$. Statistical analysis was performed using the non-parametric Kruskal–Wallis test with Dunn's post-test correction for multiple comparisons.

Rapid secretion of antimicrobials by endometrial $CD1a^+$ and $CD14^+$ selected cells in response to HIV stimulation

To further evaluate the antiviral innate responses that occur immediately after mucosal DCs encounter HIV, we analyzed the secretion of antimicrobials by FRT DCs. Purified $CD1a^+$ or $CD14^+$ cells from the EM were stimulated with HIV-BaL for 3 h prior to secretion analysis for the presence of a range of antimicrobials with known anti-HIV activity. For these studies, we used a sensitive multiplex assay developed for simultaneous detection of diverse anti-HIV molecules in small volumes to allow studies with limited cell numbers.[30] Under these conditions, we were only able to recover $CD1a^+$ and $CD14^+$ cells from the EM in sufficient numbers to perform HIV stimulation studies.

Of seven antimicrobials tested, endometrial $CD1a^+$- and $CD14^+$-selected cells constitutively produced elafin, CCL5 (RANTES), secretory leukocyte peptidase inhibitor (SLPI) and CCL20 (MIP3α) (**Figure 8a**; black points). HBD2 and HBD3 were undetectable and lactoferrin could not be evaluated because of high background concentrations in the culture media (not shown). Following HIV stimulation, significant increases in secreted elafin ($P<0.004$), CCL5 ($P<0.0008$), and SLPI ($P<0.004$) were observed within 3 h (**Figure 8a**; open points). However, when the same cells were maintained in culture for 21 additional hours following removal of the 3 h conditioned media, differences were undetectable (**Figure 8b**), suggesting that the effects observed were due to rapid release of preformed molecules.

To determine whether $CD1a^+$ and $CD14^+$ cells responded similarly to HIV stimulation, we normalized the data according to cell number and compared baseline production of the different molecules (**Figure 8c**) and responses after HIV stimulation (**Figure 8d**). Compared with $CD14^+$ cells, baseline secretion of SLPI was significantly higher in CD1a-selected cells ($P=0.015$) as well as a trend for greater CCL5 production ($P=0.06$), with no detectable differences for elafin or CCL20. Upon HIV exposure, compared to $CD14^+$ cells, $CD1a^+$ cells displayed a stronger upregulation of elafin (threefold vs 1.6-fold; $P=0.016$) and a trend for SLPI (1.9-fold vs 1.4-fold; $P=0.06$), but $CD1a^+$ and $CD14^+$ cells upregulated CCL5 equally (6.8-fold vs 5.5-fold).

As CD1a-selected cells expressed more CCR5 than CD14 selected, we evaluated the contribution of CCR5 binding to antimicrobial release by using HIV-1-BaL gp120, to try to identify the mechanism triggering secretion. Selected cells were treated with gp120 for 3 h, but no differences were found between treated and untreated cells, suggesting that the mechanism was not mediated through CCR5 (**Figure 8e**).

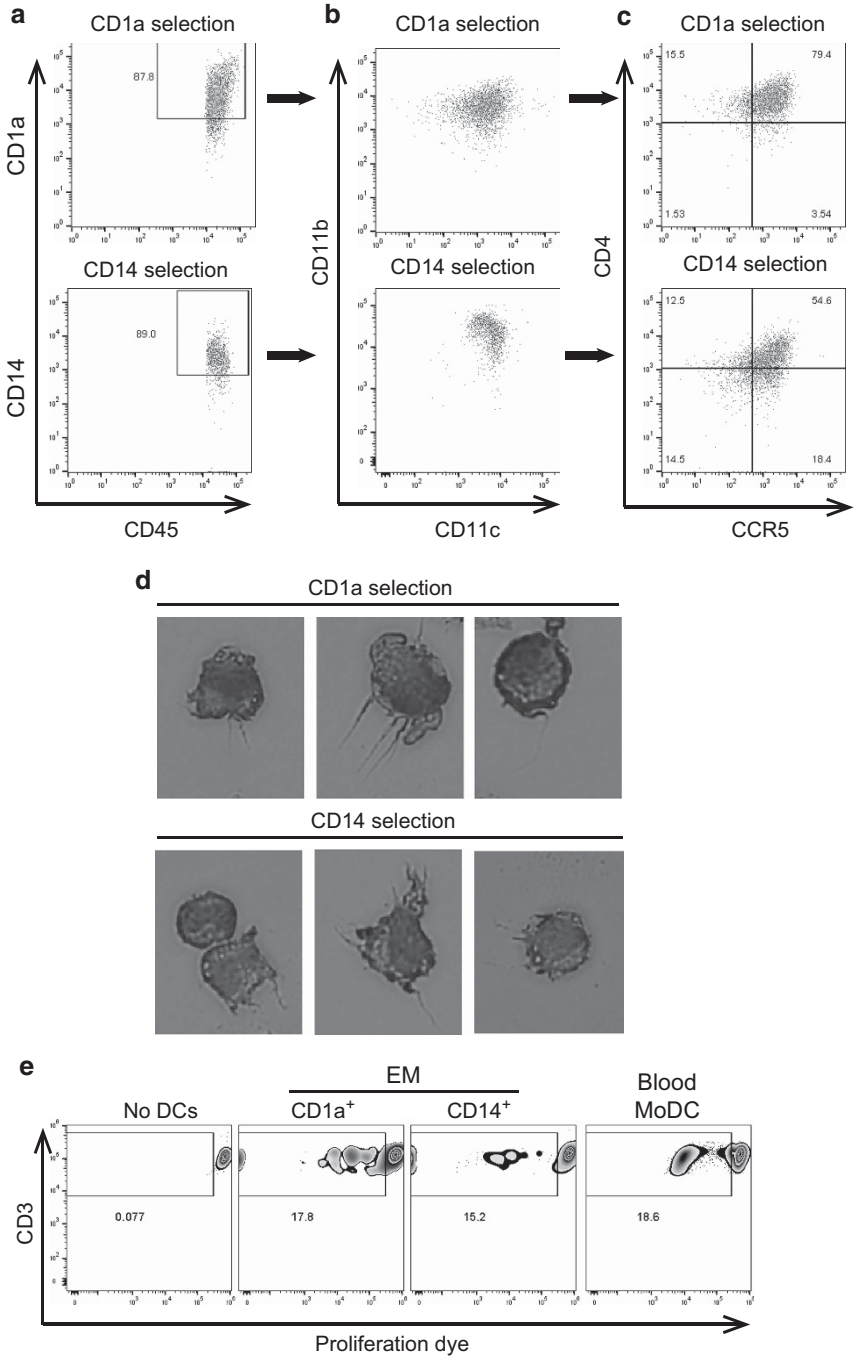

Figure 6 Characterization of CD1a$^+$ and CD14$^+$ bead selected cells. (**a**) Representative example of purity (**b**) CD11c and CD11b expression and (**c**) CD4 and CCR5 expression on EM cells after CD1a$^+$ (top) or CD14$^+$ (bottom) magnetic bead selection (representative of $n = 11$). (**d**) Morphological characteristics of the isolated cells after Giemsa staining (representative of $n = 2$). (**e**) Proliferation of blood naive T cells after allogeneic stimulation with endometrial DCs (CD1a and CD14 selection) or with *in vitro* generated monocyte-derived DCs (blood MoDCs). Representative of five different experiments with five different women.

E_2 suppresses HIV stimulated secretion of elafin and SLPI

Recognizing that E_2 modulates innate immune responses in MoDCs,[16,17] we evaluated the potential effects of E_2 on mucosal DC anti-HIV responses. Isolated DCs were pre-treated with E_2 overnight (24 h) and then exposed to HIV for 3 h. As shown in **Figure 9**, pre-treatment of the cells with E_2 prevented the induction of elafin and SLPI that was observed in the absence of E_2 ($P = 0.01$). In contrast, CCL5 was still significantly upregulated in the presence of E_2 ($P = 0.01$), although with reduced secretion levels. No effects were observed for CCL20 (not shown).

DISCUSSION

In the present study, direct comparison of DC subsets from human EM, CX and ECX demonstrates that: (1) DCs at each anatomical site display unique cell phenotypes; (2) DCs with

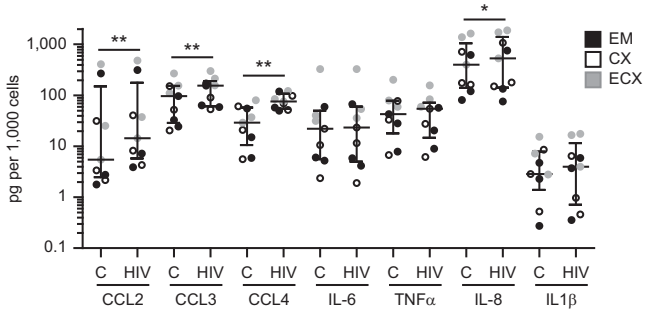

Figure 7 Secretion of cytokines and chemokines after HIV challenge of $CD14^+$ cells from EM, CX, and ECX. Secretion levels (pg per 1000 cells) after 3 h stimulation with HIV of $CD14^+$ cells from EM (black dots), CX (open circles), and ECX (gray dots). Matched EM, CX, and ECX were obtained from three different women. Statistical analysis was performed using the paired non-parametric Wilcoxon signed Rank test. Horizontal lines represent the median ± IQR. $^*P<0.05$; $^{**}P<0.01$.

the ability to capture HIV display a specific phenotype ($CD14^+$ $CD103^-$) and are present throughout the FRT and (3) HIV exposure induces rapid release of chemokines and innate anti-HIV molecules by FRT DCs. To the best of our knowledge, this study is the first to comprehensively analyze and compare DCs from different anatomical compartments in the FRT. As HIV can reach all the anatomical regions of the FRT, characterization of the DCs present at each site of HIV entry is basic information necessary for the development of preventive vaccines and microbicides.

A main conclusion in our study is that the majority of DCs present throughout the FRT are $CD11b^+CD14^+$. This finding was unexpected considering that conventional DCs are regarded as $CD14^-$ cells based on studies with blood DCs.[31] $CD14^+$ DCs have been described in human skin, where they are involved in the development of antibody responses,[32] and in the human vagina, where they have the ability to polarize naive $CD4^+$ T cells toward Th1 *in vitro*.[18] The present study extends these findings by demonstrating that $CD14^+$ DCs are the main resident DC population at all mucosal FRT sites analyzed and that they may be relevant for HIV capture as discussed below.

There is on-going controversy as to whether $CD14^+$ DCs represent bona fide DCs or monocyte-derived cell with high plasticity able to display DC or macrophage functions.[33] In our study, the majority of $CD11c^{hi}CD11b^+CD14^+$ cells co-expressed CD1c (myeloid DC marker) and lacked CD163 expression (macrophage marker). In addition, we demonstrate induction of naive T-cell proliferation by mucosal $CD14^+$-selected cells, a unique characteristic of DCs. These results are consistent with populations of $CD1c^+CD14^+$ cells found in the vagina[18] and likely represent an example of the critical influence of the mucosal environment on DC differentiation.[33] Nevertheless, the large numbers of $CD14^+CD1c^-$ cells also found in our study, likely indicate that the $CD14^+$ population represents a mixture of DCs and monocyte-derived cells. Further investigation is needed to address this issue.

Another major finding of our study is the fundamental difference in DC phenotype between EM, CX, and ECX. The most striking difference regarding phenotype was that $CD103^+$ DCs were found selectively in the EM. To the best of our knowledge, this is the first time that $CD103^+$ DCs have been identified in human EM. Others have reported the absence of $CD103^+$ DCs in ECX and vagina[18,20] but here, by performing side-by-side comparisons, we were able to characterize these cells in the human EM. This selective distribution is likely dependent on the mucosal environment, as different studies demonstrate that local production of GM-CSF regulates CD103 expression on murine DCs.[22] In this context, the preferential presence of $CD103^+$ DCs in the EM could be partially explained by increased GM-CSF production by endometrial epithelial cells relative to that seen with cervical epithelial cells.[34] Of note, we observed that T cells from the same donors expressed equivalent levels of CD103 among tissues, suggesting that CD103 expression on DCs and T cells is regulated by different mechanisms in the FRT.

The function of $CD103^+$ DCs in the human EM remains to be determined. In the human intestine, $CD103^+$ DCs represent a critical subset for the induction of regulatory T cells and oral tolerance in the steady state.[35,36] In addition, murine models demonstrate that hepatic and pulmonary $CD103^+$ DCs are required for the induction of $CD8^+$ T cell responses to viral infections.[37,38] Interestingly, pulmonary $CD103^+$ DCs are specialized in the capture and presentation of antigens derived from apoptotic cells.[39] A recent study also demonstrated that murine endometrial $CD103^+$ DCs promote T regulatory cell proliferation in response to inactivated *Chlamydia trachomatis*.[40] Whether human endometrial $CD103^+$ DCs have a role in inducing regulatory responses, presentation of apoptotic cell-derived antigens, or CD8 T-cell responses to viral infections remains to be determined. The differential distribution of $CD103^+$ DCs we found between EM, CX, and ECX is consistent with the need for tolerance and induction of regulatory T-cell responses in the EM, the site of implantation and gestation, both prior to and during pregnancy. Interestingly, we recently demonstrated that Th17 cells were significantly reduced in the EM compared to CX and ECX.[6] If endometrial $CD103^+$ DCs drive naive T cells to become regulatory T cells instead of Th17 cells, the selective presence of this DC population in the EM could be related to the relative absence of Th17 cells. The present studies begin to unravel the very unique immune cell environment in the EM.

Another profound phenotypical difference found in our study involved DC-SIGN expression. In contrast to CD103, $DC\text{-}SIGN^+$ DCs were identified in the three anatomical sites analyzed. $DC\text{-}SIGN^+$ DCs have been previously described by different studies in cervix and vagina.[19,20,41,42] Unlike other studies, our studies with matched tissues from the same patient indicate that DC-SIGN expression was significantly higher on DCs in the CX compared with EM and ECX. Previous studies from our group demonstrated that TGF-β present in conditioned media from endometrial epithelial cells was able to downregulate DC-SIGN expression on MoDCs.[43] These findings suggest that decreased DC-SIGN expression observed on endometrial DCs in the present study could be due to the

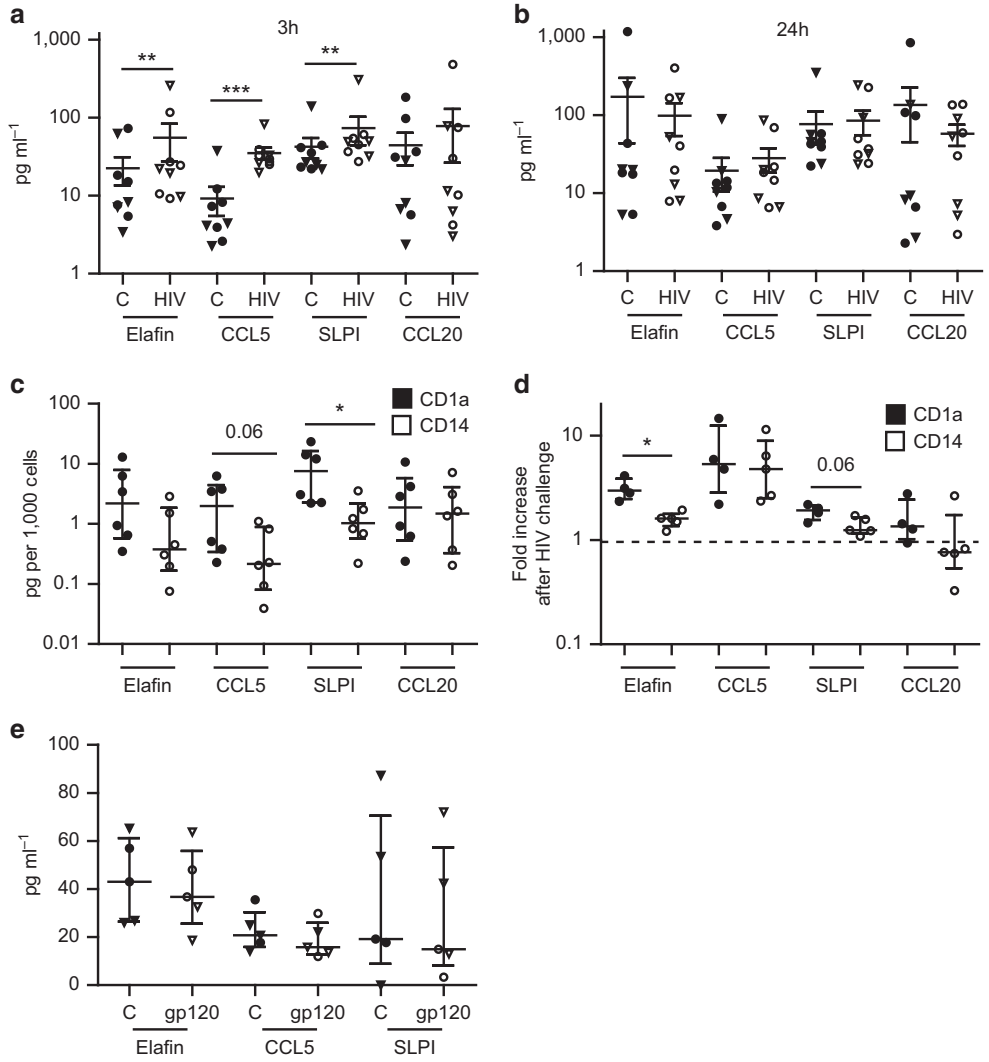

Figure 8 Secretion of antimicrobials after HIV stimulation of CD1a$^+$- and CD14$^+$-selected cells from the endometrium. (**a**) Secretion levels (pg ml^{-1}) of elafin, CCL5 (RANTES), SLPI, and CCL20 in the absence of HIV stimulation (black points; C = control) or after 3 h of stimulation with HIV (white points). (**b**) Secretion levels by the same cells shown in (**a**) 21 h after removing the initial 3 h supernatants. Results from cells selected using CD1a (triangles; $n = 4$) or CD14$^+$ (circles; $n = 5$) magnetic beads are shown combined. (**c**) Baseline secretion levels at 3 h adjusted by cell number (pg per 1000 cells), produced by CD1a$^+$-selected cells (black dots; $n = 6$) or CD14$^+$-selected cells (white dots; $n = 6$). (**d**) Fold increase in secretion levels after HIV challenge, normalized to their own control under no HIV stimulation (control = 1, dash line) for CD1a-selected (black dots; $n = 4$) and CD14-selected cells (white dots; $n = 5$) (**e**) Lack of stimulatory effect of gp120 at 3 h for the secretion of elafin, CCL5 or SLPI ($n = 5$). Each dot represents a single patient (EM). Horizontal lines represent the median ± IQR. *$P < 0.05$; **$P < 0.01$; ***$P < 0.001$. Statistical analysis was performed using the paired non-parametric Wilcoxon signed Rank test (**a**, **b** and **e**) and the non-parametric Mann–Whitney *U*-test (**c** and **d**).

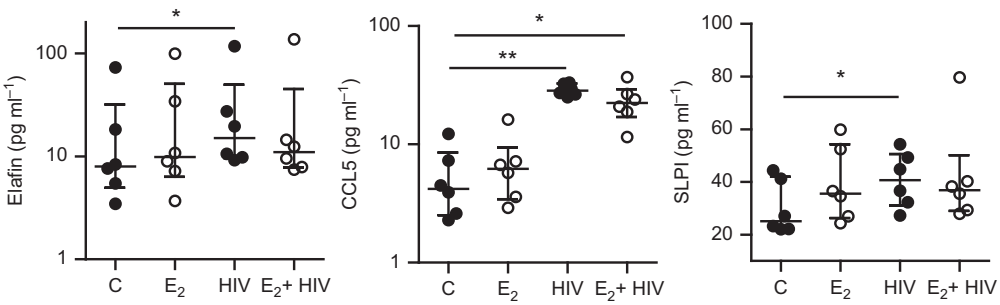

Figure 9 Effect of E_2 on elafin, CCL5, and SLPI secretion by DCs in response to HIV. Secretion levels of elafin, CCL5 and SLPI after pre-treatment with E_2 prior to HIV stimulation for 3 h (white dots) compared with production in the absence of E_2 (black dots). Results from DCs selected using CD1a or CD14$^+$ magnetic beads are shown combined. Each dot represents a single patient (EM; $n = 6$). Horizontal lines represent the median ± IQR. *$P < 0.05$; **$P < 0.01$. Statistical analysis was performed using the non-parametric Friedman test with Dunn's post-test correction for multiple comparisons.

effect of TGF-β present in the endometrial environment. We also observed expression of CD207 (langerin) only on $CD1c^+$ DCs and preferentially in the EM. A recent study demonstrated that TGF-β is also responsible for upregulation of CD207 (Langerin) on $CD1c^+$ DCs and that these cells are different from Langerhans Cells.[24]

Our studies demonstrate that $CD14^+CD103^-$ cells display HIV capture potential, and that within the cells that capture the virus, ~30% were $CD1c^+$ myeloid DCs throughout the FRT. These results suggest that the EM, in addition to the CX and ECX, is a potential site for HIV acquisition. Even though $CD4^+$ T cells in the EM are poorly susceptible to HIV-infection,[6] the presence of DCs with the ability to capture virus and potentially migrate and infect $CD4^+$ T cells in the regional lymph nodes suggests an under-appreciated uterine portal of entry for HIV and viral dissemination. Unexpectedly, we found that whereas some DCs expressed DC-SIGN, the majority that captured HIV did not express DC-SIGN. Further, the increased presence of DC-$SIGN^+$ DCs in CX did not correlate with increased viral capture in this anatomical site. Our results are in agreement with a previous report showing that HIV internalization by vaginal Langerhans cells was only marginally reduced after blockade of C-type lectin receptors.[3] The importance of DC-SIGN in HIV capture and trans-infection of T cells has been demonstrated previously using MoDCs and primary DC-$SIGN^+$ DCs from rectum and skin,[44–47] but studies comparing primary DC-$SIGN^+$ DCs from different FRT sites were lacking until now. Moreover, these results suggest that receptors other than DC-SIGN may be involved in HIV acquisition in the FRT.

In the present study we demonstrate that resident DCs in the FRT mucosa can be found with different levels of maturation. We found that HLA-DR expression was highest on ectocervical DCs, suggesting an increased general maturation status, perhaps mediated by the larger microbial load known to be present in the lower FRT. Although we did not perform migration and trans-infection assays, based on studies by others demonstrating that CCR7 is involved in cell migration to lymph nodes, and that $CD1c^+$ DCs are migratory, we speculate that a proportion of the DCs that capture HIV in the FRT have the potential to transport virus to lymphoid tissues. However, we cannot exclude the possibility that movement may be to adjacent sites in the reproductive tract rich in lymphoid aggregates.[48] It is worth noting that the expression levels of CCR7 in FRT DCs found in the present study were low compared with those reported by others in the intestinal tract.[23] This could reflect that DCs in the FRT may have impaired or limited migration potential to lymph nodes or that this function is under tighter control in the FRT.[49] Conversely, another portion of the cells that captured the virus, which lack CCR7 expression (i.e., $CD14^{hi}$), would remain in the tissue and potentially contribute to local infection. Further studies are needed to evaluate migration and HIV trans-infection properties of specific FRT DC subsets. Even though $CD14^-$ DCs are not involved in direct viral capture, their role in HIV acquisition deserves further investigation, as we demonstrate that they are responsive to HIV stimulation as discussed below. Future studies will address this issue and the implications for HIV acquisition and dissemination.

Our study demonstrates that in response to HIV, within 3 h, mucosal DCs secrete CCR5 ligands and other chemokines (CCL2, IL-8) and a spectrum of innate anti-HIV molecules, but not the classical pro-inflammatory cytokines, interferon–α2 or IL-10. Studies until now have focused on intracellular innate immune pathways or analyzed later time points after HIV exposure of MoDCs, so these acute responses have been missed. We demonstrate for the first time that elafin and SLPI are constitutively expressed in FRT DCs, and that in response to HIV exposure, both are rapidly secreted along with CCR5 ligands and other chemokines. Our findings that DCs in the FRT secrete SLPI and elafin, which are anti-proteases with anti-inflammatory and chemoattractant properties,[50] indicate an additional level of protection against HIV acquisition that is not widely recognized. Both molecules display anti-HIV activity *in vitro* by actions on target cells[51,52] or direct viral inactivation[53] for SLPI and elafin, respectively. Furthermore, the presence of SLPI and elafin in genital secretions is associated with protection against HIV acquisition.[54,55] In contrast, the presence of CCL5 in genital secretions has been associated with increased HIV acquisition[54] despite its demonstrated anti-HIV activity *in vitro*, possibly owing to chemoattraction of $CCR5^+$ $CD4^+$ T cells, the most HIV-susceptible target cells present in the human FRT as reported previously by others and us.[6,9,56–59] Therefore, whether the secretion levels of the different chemokines, elafin, and SLPI found in the present study would primarily serve an anti-HIV, anti-inflammatory, or cell recruitment function *in vivo* is difficult to predict.

Previous studies using MoDCs demonstrated that HIV specifically inhibits innate immune responses (interferon production), establishing the concept that HIV dampens innate immunity in DCs to facilitate infection.[60,61] Our results with mucosal DCs complement this information by showing that secreted innate immunity is triggered rapidly in response to viral exposure. Therefore, innate alarms and cascades for activation of surrounding cells and/or recruitment of target cells to the site of viral entry are already in place before suppression of other innate responses takes place.

We found that the rapid antiviral response of DCs was suppressed by pre-treatment with E_2, specifically the anti-inflammatory component of the response (i.e., elafin and SLPI). This suppressive activity could result in either decreased or increased susceptibility to HIV acquisition. The mechanisms that could increase HIV acquisition would be decreased secretion of SLPI and elafin, with consequent reduced anti-HIV activity, or increased mucosal activation owing to reduction of the anti-inflammatory component of the response. Immune activation has been shown in SLPI knockout mice whose DCs release more pro-inflammatory cytokines and induce enhanced proliferation of T cells.[62] Alternatively, the mechanism for decreased risk of infection after reduced SLPI and elafin production by E_2 could be due to decreased target cell recruitment. How important each of these components will be in the overall response remains to be elucidated. Consistent

with the suppressive effect of E_2 observed here, a previous study demonstrated decreased α-defensins 1–3 production by blood DCs in response to E_2 treatment, but not to progesterone (P).[16] Although P effects were not addressed here due to limited cell numbers, the roles that P and E_2/P in combination may have in anti-HIV responses deserves further investigation considering the multiple studies suggesting that high levels of P increase susceptibility to HIV infection.[9–11,63]

In conclusion, we demonstrate that DCs in the different anatomical compartments of the FRT are phenotypically distinct with differential viral capture properties, but they all rapidly respond to HIV with innate secreted molecules. Our results are relevant for rational design of microbicides and vaccines to prevent sexual transmission of HIV.

METHODS

Study subjects. Written informed consent was obtained before surgery from HIV-negative women undergoing hysterectomies at Dartmouth-Hitchcock Medical Center (Lebanon, NH, USA). Studies were approved by Dartmouth College Institutional Review Board and the Committee for the Protection of Human Subjects. Surgery was performed to treat benign conditions including fibroids, prolapsed, and menorraghia. Hormonal contraceptives were not administered before surgery. Trained pathologists selected tissue samples from EM, CX, and ECX free of pathological lesions and distant from the sites of pathology. Women were HIV − and HPV − but no additional information regarding other genital infections was available. Characteristics of the women included in the study are shown in **Table 1**.

Tissue processing. Matched tissues from the EM, CX, and ECX of the same patient were used for all experiments, except for antimicrobial production studies in response to HIV stimulation, for which enough cells could only be isolated from the EM. In some cases, only endometrial tissue was provided by pathology. Vaginal tissues were not available. Tissues were processed to obtain a stromal cell suspension as described previously,[6] using 0.05% collagenase type IV (Sigma-Aldrich, St Louis, MO, USA) and 0.01% DNAse (Worthington Biochemical, Lakewood, NJ, USA). After filtering through a 20 μm mesh screen (Small Parts) to separate epithelial cells from stromal cells, stromal cells were further purified by standard Ficoll density gradient centrifugation to remove dead cells and enrich the immune cell population before further purification. Cell preparations underwent dead cell removal (Dead Cell Removal Kit, Miltenyi biotech, San Diego, CA) as described,[6] resulting in >90% cell viability by trypan blue staining. After dead cell removal, mixed cell suspensions were used for phenotypical analyses.

Flow cytometry. Mixed cell suspensions were stained for surface markers with combinations of the following antibodies: CD45-vio-blue450, CD11b-PE (Tonbo, San Diego, CA, USA), CD11c-APC, CCR5-PE-Cy7 (BD Biosciences, San Jose, CA, USA), CCR7-PE-Cy7, HLA-DR-FITC, CD3-VioGreen (Miltenyi Biotec), CD3-APC, CD11c-PerCp-Cy5.5, CD1c-PE-dazzle, CD163-APC, HLA-DR-BV570, CD207-APC, CD1a AF700 (Biolegend), CD103-PE-Cy7, CD83-PE, CD14-e780, CD1a-FITC, CD86-e710 (eBiosciences, San Diego, CA, USA), DC-SIGN-FITC, DC-SIGN-PE, DC-SIGN-APC (R&D systems, Minneapolis, MN, USA). Dead cells were excluded with 7AAD (Southern Biotech, Birmingham, AL) or zombie dye yellow staining (Biolegend, San Diego, CA). Analysis was performed on 8-color MACSQuant 10 (Miltenyi biotech) or Gallios (Beckman Coulter, Indianapolis, IN) flow cytometers and data analyzed with FlowJo software (Tree Star, Inc. Ashland, OR). Expression of surface markers is shown as percentage of positive cells. Fluorescence minus one strategy was used to establish appropriate gates. The gating strategy is shown in **Supplementary Figure 1**.

Table 1 Characteristics of the women included in the study

	Premenopausal	Postmenopausal
Number of women	22	34
Age median (range)	43 (27-51)	60 (45-75)
Menstrual stage		
Proliferative	72.7%	
Secretory	27.3%	
Atrophic		100%

Generation of GFP-labeled VLPs. A modified pNL4-3 provirus-based plasmid for expression of GFP-labeled VLPs and encoding NL4-3 Env *in cis*, (referred to as K795) was described previously.[64] In brief, the EGFP coding sequence is expressed in frame at the 3′-end of gag, replacing the protease and most of reverse transcriptase coding region. In addition, a plasmid in which the env orf was inactivated, and from which no functional Env is expressed (referred to as K806) was derived from K795 for pseudotyping, and complemented with pBaL.26 Env expression plasmid (NIH AIDS Reagent program, Catalog Number 11446, contributed by Dr John Mascola).[65] VLPparticles, which are EGFP-labeled and non-infectious were produced by transfection, concentrated by ultracentrifugation and enumerated essentially as described.[64]

Viral capture assay. Mixed cell suspensions were incubated with HIV-GFP VLPs carrying R5env proteins at a concentration of 10 000 VLPs per cell for 1 h at 37 °C. Following incubation cells were washed to remove unbound VLPs and stained for flow cytometric analysis.

$CD14^+$ and $CD1a^+$ cell isolation and morphology. Following ficoll purification, DCs were isolated using positive magnetic bead selection with either the $CD14^+$ or $CD1a^+$ isolation kits (Miltenyi Biotec) according to the manufacturer's instructions. After two rounds of positive selection, purity of the $CD14^+$ and $CD1a^+$ population was ~90% (see **Supplementary Figure 3e**). Isolated DCs were plated (20 000–100 000 cells per well) in round-bottom ultra-low attachment 96-well plates (Corning, Corning, NY, USA) in Xvivo15 without Phenol Red (Invitrogen, Grand Island, NY) supplemented with 1% charcoal dextran-stripped human AB serum (Valley Biomedical, Winchester, VA) for *in vitro* stimulation with HIV and hormones (E_2). No changes in phenotypic markers were observed after bead selection, except for a small decrease in CD14 MFI (**Supplementary Figure 3c–e**). The rate of cell recovery per gram of tissue after magnetic selection is shown in **Supplementary Figure 3a,b**.

Cell morphology was evaluated after cytospin and Giemsa staining of CD1a and CD14 selected cells. Images were acquired using a IX73 Inverted Microscope (Olympus, Waltham, MA) with a × 40 objective.

Allogeneic naive T-cell stimulation assay. Blood naive T cells were purified after ficoll gradient using the Naive Pan T Cell Isolation Kit (Miltenyi Biotec) and stained with Cell Proliferation Dye eFluor-670 (eBioscience) as recommended by the manufacturer. Purified mucosal $CD1a^+$ or $CD14^+$ were plated with naive T cells (1:15) in round-bottom 96-well plates, in Xvivo 15 media (Invitrogen) supplemented with 10% human AB serum (Valley Biomedical). After 6 days in culture, proliferation of T cells was assessed by flow cytometry after staining with zombie yellow dye (Biolegend) and CD3-APC-Cy7 (Tonbo). As a control, blood MoDC were generated *in vitro* with IL-4 and GM-CSF[66] after $CD14^+$ selection as previously described.[16]

Hormone treatment. Immediately after isolation, $CD14^+$- or $CD1a^+$-selected cells were treated with 17β-estradiol (E_2; Sigma) for 24 h and washed before HIV exposure. E_2 was dissolved in 100%

ethanol at an initial concentration of 1×10^{-3} M prior to evaporation to dryness and resuspension in Xvivo 15 without Phenol Red (Invitrogen) media containing 1% of charcoal dextran-stripped human AB serum (Valley Biomedical) to a E_2 concentration of 1×10^{-5} M. Dilutions were made to achieve a final working hormone concentration of 5×10^{-8} M. As a control, an equivalent amount of 100% ethanol without dissolved hormone was initially evaporated. All control conditions contained evaporated ethanol as a control. Because dextran charcoal treatment of serum may introduce lipopolysaccharide contamination, expression of costimulatory molecules after incubation of cells with or without 1% charcoal-stripped human AB serum was assessed (**Supplementary Figure 2c**).

HIV and gp120 stimulation. HIV-1-BaL (R5) isolates were obtained from the AIDS Research and Reference Reagent Program, Division of AIDS, NIAID, NIH, from Dr Suzanne Gartner, Dr Mikulas Popovic, and Dr Robert Gallo[67] and propagated as described.[13] Purified $CD1a^+$ or $CD14^+$ DCs were treated with HIV-1 BaL for 3 h at a MOI of 0.5 or with 1 μg ml^{-1} of gp120 protein derived from HIV-1-BaL (NIH AIDS Reagent Program, Division of AIDS, NIAID, NIH) after which the culture supernatants were collected and stored at −80 °C until antimicrobial analysis. Media was replaced and cells kept in culture for 21 more hours after which cell supernatants were collected for antimicrobial analysis. Uninfected controls were incubated for the same length of time in media without virus or gp120.

Luminex assay. Cytokines and chemokines were measured using Millipore human cytokine multiplex kits (EMD Millipore Corporation, Billerica, MA, USA) according to the instructions. Signal was measured using the Bio-Plex array reader. Bio-Plex Manager software with five-parametric-curve fitting was used for data analysis. Molecules measured included: interferon-α2, IL-10, IL-1α, IL-1β, IL-6, IL-8, CCL2 (MCP-1), CCL3 (MIP-1α), CCL4 (MIP-1β), and tumor necrosis factor-α.

Multiplex assay. Seven different molecules known to have anti-HIV activity were evaluated in culture supernatants using a custom microsphere multiplex assay described previously.[30] In brief, commercially available antibody pairs were alternatively coupled to fluorescently coded magnetic beads to capture analyte or PE-functionalized for detection of HBD2, HBD3, elafin, SLPI, CCL5 (RANTES), CCL20 and lactoferrin. Samples were inactivated with TRITON X100, diluted 1:3 before analysis and run in triplicate.

Statistics. Data analysis was performed using the GraphPad Prism 5.0 software. A two-sided *P*-value <0.05 was considered statistically significant. Comparison of two groups was performed with the non-parametric Mann–Whitney *U*-test or Wilcoxon paired test. Comparison of three or more groups was performed applying the non-parametric Kruskal–Wallis or the paired Friedmann test followed by Dunns post-test. Data are represented as the median ± interquartile range.

SUPPLEMENTARY MATERIAL is linked to the online version of the paper at http://www.nature.com/mi

ACKNOWLEDGMENTS

We thank Dr John Fahey and Dr Yina Huang for critical comments and suggestions. We thank Richard Rossoll for technical assistance and Dr Rakesh Bakshi for help with preparing HIV-GFP VLPs. We thank the study participants, Pathologists, Obstetrics, and Gynecology surgeons, operating room nurses and support personnel at Dartmouth-Hitchcock Medical Center. Flow cytometric analysis was carried out in DartLab, the Immunoassay and Flow Cytometry Shared Resource at the Geisel School of Medicine at Dartmouth. Study supported by NIH grants AI102838 and AI117739 (CRW), CA73479 (JCK), and P30 AI27767 Birmingham Center for AIDS Research—Virology Core (CO; JCK)

AUTHOR CONTRIBUTIONS

M.R.-G., Z.S., and F.B.D. performed experiments and analyzed data; A.W.B. and M.E.A. developed the multiplex assay; J.C.K. and C.O. designed and produced HIV-GFP VLPs; M.R.-G. and C.R.W. conceived/designed the research studies and wrote the manuscript. All authors reviewed and approved the manuscript.

DISCLOSURE

The authors declare no conflict of interest.

REFERENCES

1. WHO. Progress report 2011: Global HIV/AIDS response (2011) <http://www.who.int/hiv/pub/progress_report2011/en/index.html>.
2. Nazli, A. *et al.* Exposure to HIV-1 directly impairs mucosal epithelial barrier integrity allowing microbial translocation. *PLoS Pathog.* **6**, e1000852 (2010).
3. Hladik, F. *et al.* Initial events in establishing vaginal entry and infection by human immunodeficiency virus type-1. *Immunity* **26**, 257–270 (2007).
4. Wu, L. & KewalRamani, V.N. Dendritic-cell interactions with HIV: infection and viral dissemination. *Nat. Rev. Immunol.* **6**, 859–868 (2006).
5. Wira, C.R., Rodriguez-Garcia, M. & Patel, M.V. The role of sex hormones in immune protection of the female reproductive tract. *Nat. Rev. Immunol.* **15**, 217–230 (2015).
6. Rodriguez-Garcia, M., Barr, F.D., Crist, S.G., Fahey, J.V. & Wira, C.R. Phenotype and susceptibility to HIV infection of CD4+ Th17 cells in the human female reproductive tract. *Mucosal Immunol.* **7**, 1375–1385 (2014).
7. Sallusto, F., Zielinski, C.E. & Lanzavecchia, A. Human Th17 subsets. *Eur. J. Immunol.* **42**, 2215–2220 (2012).
8. Tagliani, E. & Erlebacher, A. Dendritic cell function at the maternal-fetal interface. *Expert Rev. Clin. Iimmunol.* **7**, 593–602 (2011).
9. Saba, E. *et al.* Productive HIV-1 infection of human cervical tissue ex vivo is associated with the secretory phase of the menstrual cycle. *Mucosal Immunol.* **6**, 1081–1090 (2013).
10. Vishwanathan, S.A. *et al.* High susceptibility to repeated, low-dose, vaginal SHIV exposure late in the luteal phase of the menstrual cycle of pigtail macaques. *J. Acquir. Immune Defic. Syndr.* **57**, 261–264 (2011).
11. Kersh, E.N. *et al.* SHIV susceptibility changes during the menstrual cycle of pigtail macaques. *J. Med. Primatol.* **43**, 310–316 (2014).
12. Asin, S.N., Heimberg, A.M., Eszterhas, S.K., Rollenhagen, C. & Howell, A.L. Estradiol and progesterone regulate HIV type 1 replication in peripheral blood cells. *AIDS Res. Hum. Retroviruses.* **24**, 701–716 (2008).
13. Rodriguez-Garcia, M. *et al.* Estradiol Reduces Susceptibility of CD4(+) T Cells and Macrophages to HIV-Infection. *PLoS One* **8**, e62069 (2013).
14. Tasker, C. *et al.* 17beta-estradiol protects primary macrophages against HIV infection through induction of interferon-alpha. *Viral Immunol.* **27**, 140–150 (2014).
15. Szotek, E.L., Narasipura, S.D. & Al-Harthi, L. 17beta-Estradiol inhibits HIV-1 by inducing a complex formation between beta-catenin and estrogen receptor alpha on the HIV promoter to suppress HIV transcription. *Virology* **443**, 375–383 (2013).
16. Escribese, M.M. *et al.* Alpha-defensins 1-3 release by dendritic cells is reduced by estrogen. *Reprod. Biol. Endocrinol.* **9**, 118 (2011).
17. Escribese, M.M. *et al.* Estrogen inhibits dendritic cell maturation to RNA viruses. *Blood* **112**, 4574–4584 (2008).
18. Duluc, D. *et al.* Functional diversity of human vaginal APC subsets in directing T-cell responses. *Mucosal Immunol.* **6**, 626–638 (2013).
19. Shen, R. *et al.* Vaginal myeloid dendritic cells transmit founder HIV-1. *J.Virol.* **88**, 7683–7688 (2014).
20. Trifonova, R.T., Lieberman, J. & van Baarle, D. Distribution of immune cells in the human cervix and implications for HIV transmission. *Am. J. Reprod. Immunol.* **71**, 252–264 (2014).
21. Bogunovic, M., Mortha, A., Muller, P.A. & Merad, M. Mononuclear phagocyte diversity in the intestine. *Immunologic Res.* **54**, 37–49 (2012).
22. Merad, M., Sathe, P., Helft, J., Miller, J. & Mortha, A. The dendritic cell lineage: ontogeny and function of dendritic cells and their subsets in the steady state and the inflamed setting. *Annu. Rev. Immunol.* **31**, 563–604 (2013).
23. Mann, E.R. *et al.* Compartment-specific immunity in the human gut: properties and functions of dendritic cells in the colon versus the ileum. *Gut* **65**, 256–270 (2015).

24. Bigley, V. *et al.* Langerin-expressing dendritic cells in human tissues are related to CD1c+ dendritic cells and distinct from Langerhans cells and CD141high XCR1+ dendritic cells. *J. Leukoc. Biol.* **97**, 627–634 (2015).
25. Jensen, A.L. *et al.* A subset of human uterine endometrial macrophages is alternatively activated. *Am. J. Reprod. Immunol.* **68**, 374–386 (2012).
26. Saba, E. *et al.* HIV-1 sexual transmission: early events of HIV-1 infection of human cervico-vaginal tissue in an optimized ex vivo model. *Mucosal Immunol.* **3**, 280–290 (2010).
27. van't Wout, A.B. *et al.* Macrophage-tropic variants initiate human immunodeficiency virus type 1 infection after sexual, parenteral, and vertical transmission. *J. Clin. invest.* **94**, 2060–2067 (1994).
28. Zhu, T. *et al.* Genotypic and phenotypic characterization of HIV-1 patients with primary infection. *Science* **261**, 1179–1181 (1993).
29. Randolph, G.J., Angeli, V. & Swartz, M.A. Dendritic-cell trafficking to lymph nodes through lymphatic vessels. *Nat. Rev. Immunol.* **5**, 617–628 (2005).
30. Boesch, A.W. *et al.* A multiplexed assay to detect antimicrobial peptides in biological fluids and cell secretions. *J. Immunol. Methods.* **397**, 71–76 (2013).
31. Collin, M., McGovern, N. & Haniffa, M. Human dendritic cell subsets. *Immunology* **140**, 22–30 (2013).
32. Klechevsky, E. & Banchereau, J. Human dendritic cells subsets as targets and vectors for therapy. *Ann. N Y Acad. Sci.* **1284**, 24–30 (2013).
33. Schlitzer, A., McGovern, N. & Ginhoux, F. Dendritic cells and monocyte-derived cells: two complementary and integrated functional systems. *Semin. Cell. Dev. Biol.* **41**, 9–22 (2015).
34. Fahey, J.V., Schaefer, T.M., Channon, J.Y. & Wira, C.R. Secretion of cytokines and chemokines by polarized human epithelial cells from the female reproductive tract. *Hum. Reprod.* **20**, 1439–1446 (2005).
35. Jaensson, E. *et al.* Small intestinal CD103+ dendritic cells display unique functional properties that are conserved between mice and humans. *J. Exp. Med.* **205**, 2139–2149 (2008).
36. Coombes, J.L. & Powrie, F. Dendritic cells in intestinal immune regulation. *Nat. Rev. Immunol.* **8**, 435–446 (2008).
37. Kim, T.S. & Braciale, T.J. Respiratory dendritic cell subsets differ in their capacity to support the induction of virus-specific cytotoxic CD8+ T cell responses. *PLoS One* **4**, e4204 (2009).
38. Krueger, P.D., Kim, T.S., Sung, S.S., Braciale, T.J. & Hahn, Y.S. Liver-resident CD103+ dendritic cells prime antiviral CD8+ T cells in situ. *J. Immunol.* **194**, 3213–3222 (2015).
39. Desch, A.N. *et al.* CD103+ pulmonary dendritic cells preferentially acquire and present apoptotic cell-associated antigen. *J. Exp. Med.* **208**, 1789–1797 (2011).
40. Stary, G. *et al.* VACCINES. A mucosal vaccine against Chlamydia trachomatis generates two waves of protective memory T cells. *Science* **348**, aaa8205 (2015).
41. Jameson, B. *et al.* Expression of DC-SIGN by dendritic cells of intestinal and genital mucosae in humans and rhesus macaques. *J. Virol.* **76**, 1866–1875 (2002).
42. Duluc, D. *et al.* Dendritic cells and vaccine design for sexually-transmitted diseases. *Microbial Pathogenesis* **58**, 35–44 (2013).
43. Ochiel, D.O. *et al.* Uterine epithelial cell regulation of DC-SIGN expression inhibits transmitted/founder HIV-1 trans infection by immature dendritic cells. *PLoS One* **5**, e14306 (2010).
44. Gurney, K.B. *et al.* Binding and transfer of human immunodeficiency virus by DC-SIGN+ cells in human rectal mucosa. *J.Virol.* **79**, 5762–5773 (2005).
45. Reece, J.C. *et al.* HIV-1 selection by epidermal dendritic cells during transmission across human skin. *J. Exp. Med.* **187**, 1623–1631 (1998).
46. de Witte, L., Nabatov, A. & Geijtenbeek, T.B. Distinct roles for DC-SIGN+-dendritic cells and Langerhans cells in HIV-1 transmission. *Trends Mol. Med.* **14**, 12–19 (2008).
47. Cavarelli, M., Foglieni, C., Rescigno, M. & Scarlatti, G. R5 HIV-1 envelope attracts dendritic cells to cross the human intestinal epithelium and sample luminal virions via engagement of the CCR5. *EMBO Mol. Med.* **5**, 776–794 (2013).
48. Yeaman, G.R. *et al.* Unique CD8+ T cell-rich lymphoid aggregates in human uterine endometrium. *J. Leukoc. Biol.* **61**, 427–435 (1997).
49. Collins, M.K., Tay, C.S. & Erlebacher, A. Dendritic cell entrapment within the pregnant uterus inhibits immune surveillance of the maternal/fetal interface in mice. *J. Clin. invest.* **119**, 2062–2073 (2009).
50. Drannik, A.G., Henrick, B.M. & Rosenthal, K.L. War and peace between WAP and HIV: role of SLPI, trappin-2, elafin and ps20 in susceptibility to HIV infection. *Biochem. Soc. Trans.* **39**, 1427–1432 (2011).
51. McNeely, T.B. *et al.* Secretory leukocyte protease inhibitor: a human saliva protein exhibiting anti-human immunodeficiency virus 1 activity in vitro. *J. Clin. invest.* **96**, 456–464 (1995).
52. McNeely, T.B. *et al.* Inhibition of human immunodeficiency virus type 1 infectivity by secretory leukocyte protease inhibitor occurs prior to viral reverse transcription. *Blood* **90**, 1141–1149 (1997).
53. Ghosh, M. *et al.* Trappin-2/Elafin: a novel innate anti-human immunodeficiency virus-1 molecule of the human female reproductive tract. *Immunology* **129**, 207–219 (2010).
54. Morrison, C. *et al.* Cervical inflammation and immunity associated with hormonal contraception, pregnancy, and HIV-1 seroconversion. *J. Acquir. Immune Defic. Syndr.* **66**, 109–117 (2014).
55. Gonzalez, S.M. *et al.* High expression of antiviral proteins in mucosa from individuals exhibiting resistance to human immunodeficiency virus. *PLoS One* **10**, e0131139 (2015).
56. Joag, V.R. *et al.* Identification of preferential CD4 T-cell targets for HIV infection in the cervix. *Mucosal Immunol.* **9**, 1–12 (2015).
57. Kaul, R. *et al.* Genital levels of soluble immune factors with anti-HIV activity may correlate with increased HIV susceptibility. *AIDS* **22**, 2049–2051 (2008).
58. McKinnon, L.R. *et al.* Characterization of a human cervical CD4+ T cell subset coexpressing multiple markers of HIV susceptibility. *J. Immunol.* **187**, 6032–6042 (2011).
59. Rodriguez-Garcia, M., Patel, M.V. & Wira, C.R. Innate and adaptive anti-HIV immune responses in the female reproductive tract. *J. Reprod. Immunol.* **97**, 74–84 (2013).
60. Harman, A.N. *et al.* HIV infection of dendritic cells subverts the IFN induction pathway via IRF-1 and inhibits type 1 IFN production. *Blood* **118**, 298–308 (2011).
61. Harman, A.N. *et al.* HIV blocks interferon induction in human dendritic cells and macrophages by dysregulation of TBK1. *J.Virol.* **89**, 6575–6584 (2015).
62. Samsom, J.N. *et al.* Secretory leukoprotease inhibitor in mucosal lymph node dendritic cells regulates the threshold for mucosal tolerance. *J. Immunol.* **179**, 6588–6595 (2007).
63. Wira, C.R. & Fahey, J.V. A new strategy to understand how HIV infects women: identification of a window of vulnerability during the menstrual cycle. *AIDS* **22**, 1909–1917 (2008).
64. Forthal, D.N. *et al.* IgG2 inhibits HIV-1 internalization by monocytes, and IgG subclass binding is affected by gp120 glycosylation. *AIDS* **25**, 2099–2104 (2011).
65. Li, Y. *et al.* Characterization of antibody responses elicited by human immunodeficiency virus type 1 primary isolate trimeric and monomeric envelope glycoproteins in selected adjuvants. *J.Virol.* **80**, 1414–1426 (2006).
66. Rodriguez-Garcia, M. *et al.* Increased alpha-defensins 1-3 production by dendritic cells in HIV-infected individuals is associated with slower disease progression. *PLoS One* **5**, e9436 (2010).
67. Gartner, S. *et al.* The role of mononuclear phagocytes in HTLV-III/LAV infection. *Science* **233**, 215–219 (1986).